PAPER

Check for updates

Contrast enhanced sonothrombolysis using streptokinase loaded phase change nano-droplets for potential treatment of deep venous thrombosis†

Usama Masood,[a] Ramish Riaz,[a] Saeed Ullah Shah,[b] Ayesha Isani Majeed[c] and Shah Rukh Abbas [ID] *[a]

Current thrombolytic therapies for deep venous thrombosis are limited due to the wide side effect profile. Contrast mediated sonothrombolysis is a promising approach for thrombus treatment. The current study examines the effectiveness of *in vitro* streptokinase (SK) loaded phase–change nanodroplet (PCND) mediated sonothrombolysis at 7 MHz for the diagnosis of deep venous thrombosis. Lecithin shell and perfluorohexane core nanodroplets were prepared *via* the thin-film hydration method and morphologically characterized. Sonothrombolysis was performed at 7 MHz at different mechanical indexes of samples *i.e.*, only sonothrombolysis, PCND mediated sonothrombolysis, sonothrombolysis with SK and SK loaded PCND mediated sonothrombolysis. Thrombolysis efficacy was assessed by measuring clot weight changes during 30 min US exposure, recording the mean gray intensity from the US images of the clot by computer software ImageJ, and spectrophotometric quantification of the hemoglobin in the clot lysate. In 15 minutes of sonothrombolysis performed at high mechanical index (0.9 and 1.2), SK loaded PCNDs showed a 48.61% and 74.29% reduction of mean gray intensity. At 0.9 and 1.2 MI, 86% and 92% weight loss was noted for SK-loaded PCNDs in confidence with spectrophotometric results. A significant difference ($P < 0.05$) was noted for SK-loaded PCND mediated sonothrombolysis compared to other groups. Loading of SK inside the PCNDs enhanced the efficacy of sonothrombolysis. An increase in MI and time also increased the efficacy of sonothrombolysis. This *in vitro* study showed the potential use of SK-loaded perfluorohexane core PCNDs as sonothrombolytic agents for deep venous thrombosis.

1. Introduction

The deep vein thrombosis (DVT) is a widespread disease with complicated pathophysiology and a significant economic cost. DVT often starts without any symptoms, but it frequently leads to pulmonary emboli, which is one of the common causes of mortality in hospitalized patients.[1] Short-term anticoagulation along with heparin is the standard method of treatment, accompanied by long term usage of oral anticoagulants (3 to 6 months).[2,3] Nevertheless, this mode of treatment frequently fails to recanalize veins, leading to post-thrombotic syndrome and venous valve dysfunction.[4] Rapid recanalization of the vessels, according to studies, helps sustain valve competency.[5] To assure

long-term stability of the affected vessel, a treatment that stimulates active disintegration of the blockage is desired. In the more serious conditions of DVT, thrombolytic drugs (*e.g.*, streptokinase, urokinase, rt-PA) are employed, although they come with a risk of significant bleeding.[6] Mechanical thrombectomy and catheter-directed thrombolytics are also options, although they come with the same risks of pulmonary embolism and bleeding if not properly filtered.[7]

Energy of ultrasonics has been extensively studied as a means of promoting thrombolysis.[8,9] In most previous studies, ultrasonography was utilized to increase the efficacy of a thrombolytic drug or as a means of mechanical thrombectomy utilizing a catheter-based device.[10] *In vitro* and *in vivo* models have been used to demonstrate the feasibility of these approaches.[11] Clinical studies have also shown the efficacy of ultrasound-enhanced thrombolysis, which uses low-power transcutaneous or catheter-delivered ultrasound in combination with thrombolytic medicines to treat ischemic stroke.[12,13] Along with an extracorporeal positioning, ultrasound can be targeted to a higher intensity within internal organs or vessels.

[a]Department of Industrial Biotechnology, Atta-Ur-Rahman School of Applied Biosciences (ASAB), National University of Sciences and Technology, Islamabad, Pakistan. E-mail: sabbas@asab.nust.edu.pk

[b]Department of Cardiology, Shifa International Hospitals Ltd., Islamabad, Pakistan

[c]Department of Radiology, Pakistan Institute of Medical Sciences, Islamabad, Pakistan

† Electronic supplementary information (ESI) available. See https://doi.org/10.1039/d2ra04467f

Ultrasound-induced the shear forces or cavitation bubbles can increase thrombolytic drug distribution and penetration into the clot, increasing potency.[14] However, the prolonged presence of substantial adverse effects associated with thrombolytic medicines or catheter-based mechanical thrombectomy are limits of these techniques.

Targeted transcutaneous ultrasonography is also employed in histotripsy, but no thrombolytic drugs are used. Conversely, histotripsy uses short, high-intensity ultrasound pulse to create acoustic cavitation, which causes a controlled mechanical breakup of the thrombus.[15,16] Cavitation bubbles grow and contract in response to ultrasonic pressure at the focal. The thrombus is mechanically ruptured as a result of this action, which causes high localized pressure in the thrombus.[17] Above a certain pressure threshold, a cloud of cavitation bubbles occurs near the transducer's focus,[18] inducing mechanical breakup of the thrombus in acellular detritus.[19] *In vitro*, histotripsy resulted in full disintegration of 300 mg thrombi in under 2 minutes. Approximately most of the procedure's debris had a diameter of 100 μm. The bubble cloud might be seen as a dynamic, hyperechoic zone on ultrasound imaging, providing real-time feedback on therapeutic progress and efficacy.[20] The technique has been employed in treatment of deep venous thrombosis also. Maxwell *et al.* conducted a study and utilized 1 MHz focused transducer and used 14 to 19 MPa waves for treatment DVT in porcine model and visualized it *via* 8 MHz probe.[21]

Catheter directed thrombolysis is also an effective way of treating deep venous thrombosis. In catheter directed thrombolysis, catheter is advanced to the blocked vessel and thrombolytic drug is directly infused to the affected area. Catheter mediated sonothrombolysis is more advanced technique merging sonothrombolysis *via* forward looking intravascular transducers and administration of anticoagulants.[22] The efficacy is further enhanced by microbubble/nanodroplet administration. Use of microbubble contrast agents lowers the threshold of cavitation.[23] They accelerate the thrombolysis by creating localized mechanical stress in thrombus. Loading of microbubbles with anti-thrombolytic agents can further increase the thrombolytic efficiency while decreasing the systemic side effects of anti-thrombolytic therapy by local release of drug.[24] Multiple *in vivo* studies on microbubble mediated sonothrombolysis has shown its potential in treating thrombosis of different regions including illio-femoral arteries, coronary arteries and cerebral vessels.[25–27]

Compared to microbubbles phase convertible nanodroplets are proved to be safer and more effective in sonothrombolysis. Due to their small size they are able to penetrate more in clots compared to microbubble. Also they create debris of smaller size resulting in less chanced of embolism.[28] Recently Goel *et al.* studied the effect of nanodroplets mediated catheter directed sonothrombolysis for retracted clots and founds significantly high lysis effect for phase change nanodroplets compared to microbubbles.[29]

The diagnostic frequency range utilized for imaging DVT of extremities lie between 5 and 10 MHz frequency with mechanical index (MI) range of 0.1 to 1.5.[30] The FDA approved limit for safe use of ultrasound allows MI of 1.9 corresponding to 5 MPa. Therefore, majority of clinical scanner have MI range of 0.1 to 1.5 MI corresponding to 0.81 MPa to 5 MPa at 7.5 MHz frequency. Currently studies are focused on designing such constructs which break clot in diagnostic MI range especially for middle cerebral artery (MCA).[24] Commercially available contrast agents are designed for low frequency applications and usually respond best between 2 and 5 MHz frequency range and are in study for sonothrombolysis of MCA. For theragnostic application of DVT, microbubbles must be able to perform at higher frequencies as diagnosis of both upper and lower extremity DVT is usually done *via* linear probes having frequency range of 5 to 10 MHz.[23]

Herein, we synthesized perfluorohexane loaded PCNDs and used them for contrast mediated sonothrombolysis due to its higher acoustic droplet vaporization (ADV) and ability to perform at higher frequencies.[31] We built an *in vitro* model of DVT and intended to cure thrombi by diagnostic ultrasound at mechanical indices ranging from 0.1 to 1.2 corresponding to 0.83 to 4.05 MPa. Clots were produced in the polyurethane tube for our research model, simulating human thrombi, and the thrombus was detected and targeted fully through ultrasonic imaging at 7.5 MHz.

2. Experimental

Study was approved by NUST Ethical Review Committee. Blood from healthy volunteers was taken after informed verbal consent for making *in vitro* thrombus model. None of the experiments involved any *in vivo* experimentation.

2.1. Materials

Chloroform and Tween 80 were purchased from Sigma Aldrich, cholesterol from Scharlau, and perfluorohexane (PFH) from Shanghai Tianfu. SK (Streptase® 1.5M IU) was provided as a gift from Shifa International Hospital solely for research purposes.

2.2. Synthesis of PCNDs

Firstly, perfluorohexane emulsion was prepared by taking 10 ml of 2.5% solution of Tween 80 in PBS and adding 0.5 ml of PFH drop by drop on a magnetic stirrer until the PFH is dissolved. PCNDs were prepared by the method of thin-film hydration. For this 50 mg of the soy lecithin and 10 mg of the cholesterol were dissolved in chloroform. Chloroform was evaporated under the vacuum at a temperature of 50 °C in the rotary evaporator until the thin film was deposited at the round bottom flask. Thin film was dried for 1 hour under the vacuum. Deposited film was rehydrated with the 10 ml of prepared PFH emulsion and heated above the transition temperature of the soy lecithin ($T_m = 50 °C$) for encapsulation of PFH within soya lecithin. For SK loaded PCNDs, thin film was rehydrated with the SK containing emulsion. SK emulsion was prepared *via* dropwise addition of both SK and PFH in solution of 2.5% Tween 80 and PBS upon continuous stirring. The PCNDs suspension was than extruded three times to reduce the size of

the PCNDs followed by centrifugation at 6000 rpm. For extrusion, PCNDs were passed through 0.4 μm membrane filter under vacuum filtration.

2.3. Drug encapsulation efficiency

UV visible spectrophotometer (Analytik Jena Germany, Model: SPECORD 200 Plus) was used for measuring the SK content in lecithin PCNDs at a specific wavelength of 278 nm. Blank utilized in the procedure was 95% ethanol to ensure the quality of results. For the quantification of the SK, the suspension should be free first from the free drug that was present in the medium. For disruption of the lecithin PCNDs, 2 ml ethanol should be added into the medium which ultimately led to drug release. Then the sample was subjected to vigorous vortex and centrifugation at 4000 rpm for 10 min to separate the lipid precipitates. Lipid was settled as pallet while the drug was collected from supernatant which was further subjected to spectrophotometric studies.[32]

To find out the SK quantity in the lecithin PCNDs, a calibration curve was drawn for SK. For this SK was dissolved in the dextrose water and make dilutions *i.e.*, range 0.1–0.5 g ml^{-1} with linear equation ($y = 2.57x + 0.265$) and used to find out concentration of the SK in the lecithin PCNDs and to find out the encapsulation efficiency of the SK in the lecithin PCNDs, to quantify the amount of the SK in the PCNDs UV absorption of the sample was recorded and compared with the calibrated curve of the SK and that experiment was performed three times and the average result values were put in the formula given below to calculate the encapsulation efficiency of SK in the PCNDs.

2.4. Preparation of *in vitro* thrombus model

For *in vitro* clot model, urinary bag tubes made up of poly urethane were used to mimic deep veins. The size of tube was 24 fr *i.e.*, 8 mm in diameter and length of 10 cm resembling femoral veins. Poly urethane tubes were chosen because of their visibility under ultrasound. The material has speed of 1700 m s^{-1}, density of 1.04 g cm^{-3} and acoustic impedance of 1.80 MRayls. Water was injected inside the tubes form both ends. Clot was developed in the center with an approx. size of 2–3 cm. PCNDs were injected from single end of tube. Tubes were clamped in container filled with water. Since water has acoustic impedance of 1.48 MRayls. Mismatch between both made the tubes and clot visible. The tubes allowed the transmission of ultrasound beam as speed of sound in both water and tube lie within soft tissue ranges of speed of sound.

A blood clot was prepared according to the method reported in the literature.[33] For this volume of 2.5 ml of 100 mM molarity of calcium, chloride solution was taken, and mixed in the 1 ml

of anticoagulated human blood that was collected from the volunteer. After 5 minutes, the mixture was injected into the poly urethane tubes while taking care to avoid the injection of air bubbles in the poly urethane tube. Then, blood containing polyurethane tubes were incubated at 37 °C for the duration of 3 hours followed by refrigeration for 3 days to allow proper retraction of the clot.

2.5. Physiochemical characterization of microbubble constructs

2.5.1. Scanning electron microscopy. The structure and the morphology of the PCNDs were analyzed using the scanning electron microscope, model: (JEOL, Japan, Model no JSM-6490LA). For this, PCNDs were sonicated and diluted, and one drop of each sample was placed on the slides followed by drying in vacuum desiccator. All samples were gold sputtered and analyzed at voltage of 10 kV.

2.5.2. Zeta potential measurements. Zeta sizer (Malvern Zeta Sizer ver 7.12, UK, Serial No. MAL1168467) was used to measure the size of the microbubble and zeta potential at the temperature of 25 °C and pH = 7.4. To analyze the sample, 20 microliters of sample was diluted in the 2 ml of distilled water. Size, and the zeta potential of the microbubble was measured in the triplicates.

2.5.3. Fourier transform infra-red spectroscopy (FTIR). For FTIR analysis, KBr pellets along with samples were made. Spectra of the samples were recorded in infrared range of 4000–350 cm^{-1} at room temperature using FTIR spectrophotometer (PerkinElmer, USA, Model: Spectrum 100).

$$\text{Encapsulation efficiency}(\%) = \frac{\text{Concentration of SK detected in medium}}{\text{Concentration of SK added initially}} \times 100$$

2.6. Acoustic setup for sonothrombolysis

The prepared clot model was subjected to the process of the sonothrombolysis under diagnostic ultrasound (Toshiba Applio 500, Japan) with PLT 805 11L4 Linear array probe (5 to 11 MHz). Following parameters were used:

• Central frequency of transducer = 7.5 MHz.
• Mechanical index of produced ultrasound (MI) = 0.1, 0.3, 0.6, 0.9 and 1.2.
• Depth = 5 cm.
• PRF-15.4 kHz.
• Frame rate = 60 fps.
• Gain = 85.
• Focus: 2 cm exactly in line with clot.

Imaging: performed in longitudinal direction with probe hanged 2 cm above clot (ESI Fig. 1†).

In this study blood clot model was exposed to ultrasound waves for 30 minutes with under different conditions *i.e.*, sonothrombolysis only (US only), PCND mediated

sonothrombolysis (US + PCNDS), sonothrombolysis with iv SK administration (US + SK), SK loaded PCNDs contrast mediated sonothrombolysis (US + SK loaded PCNDS). Sonothrombolysis of these samples was analyzed by mean gray intensity analysis of ultrasound images of the blood clot, pre and post percentage weight loss of the blood clot, and hemoglobin analysis in the clot lysate that we collected after 30 minutes of the process of the sonothrombolysis by absorption at UV visible spectrophotometer analysis.

2.6.1. Ultrasound image analysis of the clot model. Ultrasound images of the blood clot were stored during the process of the sonothrombolysis. Images were captured after every 3 minutes of sonothrombolysis for all the groups of the study. Images of the ultrasounds were analyzed with the software *i.e.*, ImageJ. Mean gray intensity of the clot of interest in ultrasound images were recorded. Region of interest and *X–Y* coordinates were kept constants for all images.

2.6.2. Weight analysis of *in vitro* clot model. All blood clots were weighed before and after sonothrombolytic treatment of 30 minutes and percentage weigh loss was calculated. Every reading was taken thrice and then mean was calculated.

2.6.3. Spectrophotometric analysis of hemoglobin of red blood cells. Effluents of clot lysis were collected absorption of hemoglobin was recorded at 405 nm wavelength in UV-vis spectrophotometer after the exposure of 30 minutes of ultrasound waves in various study groups.

3. Results and discussion

3.1. Physicochemical analysis of PCNDs

3.1.1. Size and surface charge of lecithin PCNDs. A homogenous spherical population of the lecithin microbubble concerning size can be seen in Fig. 1.

The average size of the lecithin PCNDs was 357.8 nm ± 124 in zeta sizing analysis as shown in the table. For lecithin PCNDs, the zeta potential was found to be −28.3 (mV) as shown in Table 1.

3.1.2. Fourier transform infra-red (FTIR) spectroscopy. Fourier transform infra-red (FTIR) spectroscopy was performed to analyse the important chemical functional groups and the

Table 1 Zeta potential and zeta size of lecithin PCNDs

Sample	SEM size (nm)	Zeta size (nm)	Zeta potential	PDI
Lecithin PCNDs	366.761 ± 7	357.8 ± 124	−28.5	0.149

surface chemistry of the PFH loaded lecithin microbubble. Fig. 2, yellow curve shows the FTIR of PFH which shows the stretching of carbon and fluorine (C–F) at 1250 cm^{-1}, 1180 and 1080 cm^{-1}. Soy lecithin (blue curve) had typical peaks between 3436 cm^{-1} and 755 cm^{-1}. In the area, 1770–1500 cm^{-1} were apparent vibrations of bending of hydroxyl (OH) and carbonyl (C–OH) stretches. The standard ranges observed for P=O between 1200 and 1146 cm^{-1} and P–O–C, 1446 cm^{-1} to 788 cm^{-1}. The dominant bands located at 3412 cm^{-1} to 593 cm^{-1} correspond to the pure cholesterol spectrum Fig. 2(c). The presence of OH stretches is due to the strong vibration band observed at 3408 cm^{-1}. Fig. 2, red curve shows a strong band at 3440 cm^{-1} of PFH loaded lecithin PCNDS due to its stretching of OH (strong hydrogen bonding). CH degree of absorption is due to the absorption peaks 2932-1 and 2851-1. The C=C band can be measured at 1632 cm^{-1} suggesting binding of lecithin and cholesterol. Appearance of 1250 cm^{-1} peak in PCNDs shows successful incorporation of PFH in these PCNDs. All these peaks correspond with the peaks of PCNDs reported in the literature.[34]

3.2. SK encapsulation efficiency

For the standard curve for SK, a graph was generated between the absorbance of the UV spectrophotometer and the concentrations Fig. 3. The concentration of the free SK in the supernatant was determined through this curve using the following equation.

$$y = mx + b$$

Therefore.

$$\frac{y - b}{m} = x$$

Fig. 1 SEM images of lecithin PCNDs at (a) 20000×, (b) 10 000×, 5000× and 1000×.

Fig. 2 FTIR spectrum of cholestrol, soy lecithin, perfluorohexane and perfluorohexane loaded soy lecithin PCNDs.

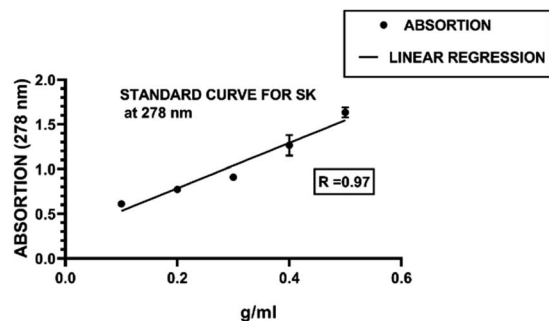© 2022 The Author(s). Published by the Royal Society of Chemistry

Fig. 3 Standard curve for SK in concentration 0.1–0.5 g ml^{-1}, for drug encapsulation efficiency analysis. Each sample was run in triplicate ($n = 3$, STD ± 0.23) and the graph was plotted against mean values.

where the variable b represents the y-intercept of the line graph. The y-intercept is the point at which the line intersects the y-axis. The variable m represents the line's slope. x is the independent variable and could be any point on the slope or our value of interest.

According to this, SK loading efficiency was found to be 64.71%.

3.3. Analysis of sonothrombolytic efficiency

3.3.1. Mean gray intensity. Ultrasound is commonly used for the diagnosis of DVT. DVT appears echogenic in dark vessel. Clot stability leads to increase in echogenicity due to deposition of fibrin. Also, larger the diameter of clot large area will result in high intensity of pixels in selected ROI region. Different AI based techniques also measure clot intensity for auto diagnosis, severity and size of thrombus.[35,36] We measured the change of mean ROI intensity as a parameter for thrombolytic efficiency.

Fig. 4(a) is showing the gradual decrease of mean gray intensity at all mechanical index (0.1, 0.3, 0.6, 0.9 and 1.2) for sonothrombolysis performed for 15 and 30 minutes with all samples. Significant difference (P-value < 0.01, ESI Table 12†) was found between 0.3 and 0.6 MI for SK loaded PCNDs which showed 66.34% and 87.27% respectively. In 15 minutes of sonothrombolysis performed at high mechanical index (0.9 and 1.2), SK loaded PCNDs 48.61% and 74.29% respectively reduction of mean gray intensity with (US + SK loaded PCNDS). Among all groups SK loaded PCNDs showed more thrombolysis than contrast only PCNDs (P-value < 0.01, ESI Table 1†).

Fig. 4(b) and (c) shows the graph between mean gray intensity and time to compare the reduction of mean gray intensity at low MI for 30 minutes of sonothrombolysis and at high MI for 15 minutes of sonothrombolysis respectively. Sonothrombolysis performed for 30 minutes with (US + SK loaded PCNDs) showed maximum reduction of mean gray intensity at mechanical index 1.2. Sonothrombolysis performed for 15 and 30 minutes with (US + PCNDS) also showed 38.77% and 58.95% reduction of mean gray intensity respectively.

Within time domain again loaded PCNDs showed more thrombolysis than contrast only PCNDs (P-value < 0.01, ESI Table 2†).
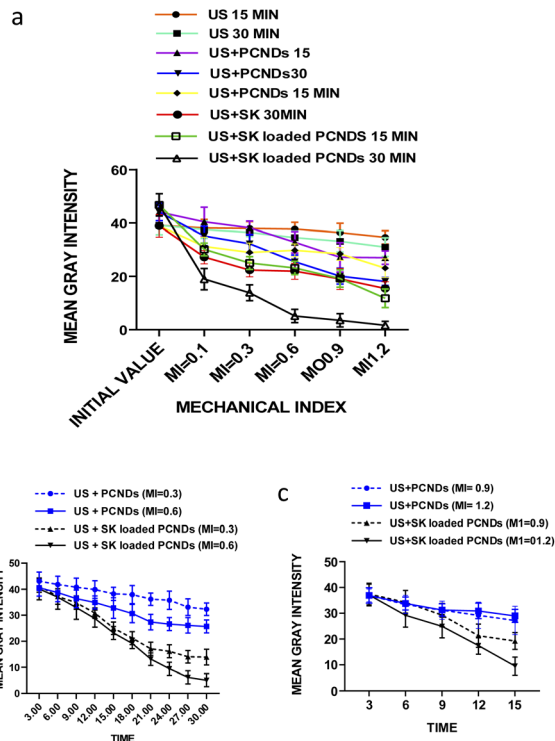

Fig. 4 Mean gray intensity analysis after sonothrombolysis at ultrasound frequency 7.5 MHz at mechanical index 0.1, 0.3, 0.6, 0.9, and 1.2 for the time of 15 and 30 minutes. (a) Showing the reduction of mean gray intensity during sonothrombolysis performed with sample (US only), (US + MB), (US + SK) and (US + SK loaded PCNDs). (b) Showing the reduction of mean gray intensity at low MI (0.3 and 0.6) with sample (US + PCNDs) and (US + SK loaded PCNDs). (c) Showing the reduction of mean gray intensity at high MI (0.6 and 1.2) with sample (US + PCNDs) and (US + SK loaded PCNDs).

These results show that loading of SK in PCNDs, increase in MI and increase in time duration increases the thrombolytic efficiency. Leeman *et al.* also observed that increase in MI from 0.6 to 1.2 and loading of rtPA increases the microbubble mediated sonothrombolytic efficiency.[37] Fig. 5 shows the original images of sonothrombolysis.

3.3.2. Weight analysis. Pre and post weight analysis were performed for assessment of percentage weight loss of blood clot model.

Weight loss analysis also showed similar results *i.e.*, at all mechanical indices, SK loaded PCNDs showed highest efficacy
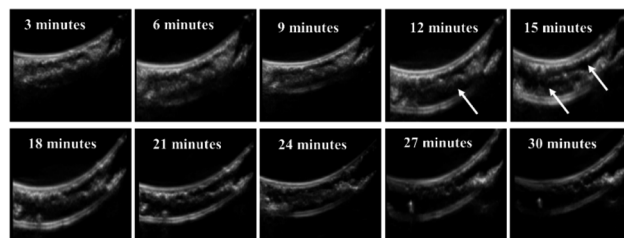

Fig. 5 US images of blood clot during sonothrombolysis at 7.5 MHz, MI 1.2 MHz with (US + SK loaded PCNDs).

for sonothrombolysis, followed by sonothrombolysis and iv SK administration, microbubble mediated sonothrombolysis and sonothrombolysis alone. ESI Table 3† shows the ANOVA results of these findings depicting the mentioned pattern.

With increase of mechanical index, percentage weigh loss increased in all the samples *i.e.*, (US only), (US + PCNDS), (US + SK) and (US + SK loaded PCNDS). Maximum percentage weight loss of thrombus was recorded when sonothrombolysis performed with (US + SK loaded PCNDS) at all mechanical index (*i.e.*, 0.1, 0.3, 0.6, 0.9 and 1.2) with percentage age weight loss of thrombus being 58%, 67%, 75%, 86% and 92% respectively (Fig. 6).

3.3.3. Spectrophotometric analysis of clot lysate. Thrombolytic efficiency was also observed *via* absorption of hemoglobin at 405 nm of clot lysate collected after the process of sonothrombolysis in all samples.
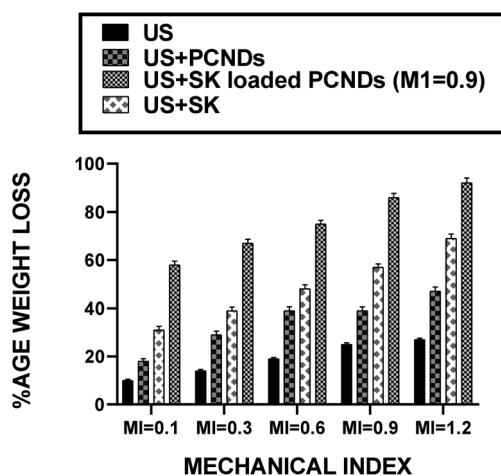
Fig. 6 Weight analysis after sonothrombolysis at US frequency 7.5 MHz at mechanical index 0.1, 0.3, 0.6, 0.9, and 1.2 with (US) only, (US + MB), (US + SK) and (US + SK loaded PCNDs).
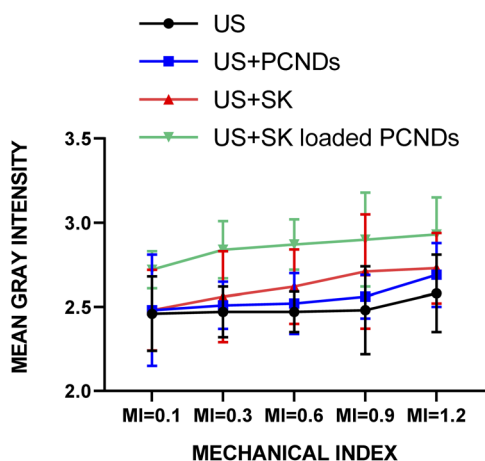
Fig. 7 Absorbance of hemoglobin at 405 nm of effluent, collected after sonothrombolysis with US frequency 7.5 MHz at MI 0.1, 0.3, 0.6, 0.9, and 1.2 with (US) only, (US + MB), (US + SK) and (US + SK loaded PCNDs).

Fig. 7 is showing a plotted graph between absorption and mechanical index. The results were similar as observed by ROI mean intensity and percentage weigh loss measurements. Maximum absorption of hemoglobin was recorded for clot lysate that were collected after the sonothrombolysis performed with SK loaded PCNDS at MI 1.2.

PCNDs contrast mediated sonothrombolysis is widely researched topic due to its safety, noninvasiveness and cost. However, majority of papers are focused on use of lower frequency probe either in kHz frequency or with 1 to 3 MHz frequency to be used for stroke imaging and thrombolysis. Also, the reason could be use of standard contrast agents in these studies like Definity, Sonovue *etc.*, all of which perform better up to 3 MHz frequency and their microbubbles destabilized at 7.5 MHz frequency.[38–40] We used PFH as core gas material which has higher ADV achieved at higher frequencies. This made our PCNDs to respond at 7.5 MHz frequency and able to perform thrombolysis at high frequency.[31,41] This make our PCNDs as excellent theranostic agent for DVT.

4. Conclusion

SK loaded PCNDs demonstrated successful sonothrombolysis at 7.5 MHz frequency therefore can be used as potential candidate for deep venous thrombosis therapy. They performed better than unloaded PCNDs or sonothrombolysis therapy alone. Thrombolytic efficiency increased with increase in MI and time.

Funding

Author contributions

Usama Masood: data curation, formal analysis, methodology, visualization, validation, writing – original draft. Ramish Riaz: data curation, formal analysis, methodology, validation. Saeed Ullah Shah: formal analysis, methodolgy. Ayesha Isani Majeed: formal analysis, methodology. Shah R Abbas: conceptualization, supervision, funding acquisition, supervision, writing – review & editing.

Conflicts of interest

There are no conflicts to declare.

Acknowledgements

References

1 G. D. Motykie, L. P. Zebala, J. A. Caprini, C. E. Lee, J. I. Arcelus, J. J. Reyna, *et al.*, A guide to venous thromboembolism risk factor assessment, *J. Thromb. Thrombolysis*, 2000, **9**(3), 253–262.

2 P. Prandoni, A. W. Lensing, H. R. Büller, A. Cogo, M. H. Prins, A. M. Cattelan, *et al.*, Deep-vein thrombosis and the incidence of subsequent symptomatic cancer, *N. Engl. J. Med.*, 1992, **327**(16), 1128–1133.

3 M. J. Sharafuddin, S. Sun, J. J. Hoballah, F. M. Youness, W. J. Sharp and B.-S. Roh, Endovascular management of venous thrombotic and occlusive diseases of the lower extremities, *J. Vasc. Intervent. Radiol.*, 2003, **14**(4), 405–423.

4 A. J. Comerota and D. J. Paolini, Treatment of acute iliofemoral deep venous thrombosis: a strategy of thrombus removal, *Eur. J. Vasc. Endovasc. Surg.*, 2007, **33**(3), 351–352.

5 M. H. Meissner, R. A. Manzo, R. O. Bergelin, A. Markel and D. E. J. Strandness, Deep venous insufficiency: the relationship between lysis and subsequent reflux, *J. Vasc. Surg.*, 1993, **18**(4), 596–598.

6 H. D. White and D. P. Chew, Acute myocardial infarction, *Lancet*, 2008, **372**(9638), 570–584.

7 M. J. Sharafuddin and M. E. Hicks, Current status of percutaneous mechanical thrombectomy. Part I. General principles, *J. Vasc. Intervent. Radiol.*, 1997, **8**(6), 911–921.

8 G. Trübestein, C. Engel, F. Etzel, A. Sobbe, H. Cremer and U. Stumpff, Thrombolysis by ultrasound, *Clin. Sci. Mol. Med., Suppl.*, 1976, **3**, 697s–698s.

9 K. Tachibana, Enhancement of fibrinolysis with ultrasound energy, *J. Vasc. Intervent. Radiol.*, 1992, **3**(2), 299–303.

10 S. Atar and U. Rosenschein, Perspectives on the role of ultrasonic devices in thrombolysis, *J. Thromb. Thrombolysis*, 2004, **17**(2), 107–114.

11 B. Devcic-Kuhar, S. Pfaffenberger, L. Gherardini, C. Mayer, M. Gröschl, C. Kaun, *et al.*, Ultrasound affects distribution of plasminogen and tissue-type plasminogen activator in whole blood clots in vitro, *Thromb. Haemostasis*, 2004, **92**(5), 980–985.

12 G. Tsivgoulis, J. Eggers, M. Ribo, F. Perren, M. Saqqur, M. Rubiera, *et al.*, Safety and efficacy of ultrasound-enhanced thrombolysis: a comprehensive review and meta-analysis of randomized and nonrandomized studies, *Stroke*, 2010, **41**(2), 280–287.

13 B. R. Mahon, G. M. Nesbit, S. L. Barnwell, W. Clark, T. R. Marotta, A. Weill, *et al.*, North American clinical experience with the EKOS MicroLysUS infusion catheter for the treatment of embolic stroke, *AJNR Am. J. Neuroradiol.*, 2003, **24**(3), 534–538.

14 M. J. Stone, V. Frenkel, S. Dromi, P. Thomas, R. P. Lewis, K. C. P. Li, *et al.*, Pulsed-high intensity focused ultrasound enhanced tPA mediated thrombolysis in a novel *in vivo* clot model, a pilot study, *Thromb. Res.*, 2007, **121**(2), 193–202.

15 M. Nadrljanski, Z. Milošević, V. Plešinac-Karapandžić and B. Goldner, The role of breast magnetic resonance imaging in the diagnosis of ductal carcinoma in situ, *Srp. Arh. Celok. Lek.*, 2013, **141**(5–6), 402–408.

16 Z. Xu, J. B. Fowlkes, A. Ludomirsky and C. A. Cain, Investigation of intensity thresholds for ultrasound tissue erosion, *Ultrasound Med. Biol.*, 2005, **31**(12), 1673–1682.

17 A. D. Maxwell, C. A. Cain, A. P. Duryea, L. Yuan, H. S. Gurm and Z. Xu, Noninvasive thrombolysis using pulsed ultrasound cavitation therapy–histotripsy, *Ultrasound Med. Biol.*, 2009, **35**(12), 1982–1994.

18 Z. Xu, J. B. Fowlkes, E. D. Rothman, A. M. Levin and C. A. Cain, Controlled ultrasound tissue erosion: the role of dynamic interaction between insonation and microbubble activity, *J. Acoust. Soc. Am.*, 2005, **117**(1), 424–435.

19 R. A. Roy, A. A. Atchley, L. A. Crum, J. B. Fowlkes and J. J. Reidy, A precise technique for the measurement of acoustic cavitation thresholds and some preliminary results, *J. Acoust. Soc. Am.*, 1985, **78**(5), 1799–1805.

20 T.-Y. Wang, Z. Xu, T. L. Hall, J. B. Fowlkes and C. A. Cain, An efficient treatment strategy for histotripsy by removing cavitation memory, *Ultrasound Med. Biol.*, 2012, **38**(5), 753–766.

21 A. D. Maxwell, G. Owens, H. S. Gurm, K. Ives, D. D. J. Myers and Z. Xu, Noninvasive treatment of deep venous thrombosis using pulsed ultrasound cavitation therapy (histotripsy) in a porcine model, *J. Vasc. Intervent. Radiol.*, 2011, **22**(3), 369–377.

22 D. Fleck, H. Albadawi, F. Shamoun, G. Knuttinen, S. Naidu and R. Oklu, Catheter-directed thrombolysis of deep vein thrombosis: literature review and practice considerations, *Cardiovasc. Diagn. Ther.*, 2017, **7**(suppl. 3), S228–S237.

23 T. Şen, O. Tüfekçioğlu and Y. Koza, Mechanical index, *Anatolian J. Cardiol.*, 2015, **15**(4), 60.

24 Y. Lu, J. Wang, R. Huang, G. Chen, L. Zhong, S. Shen, *et al.*, Microbubble-Mediated Sonothrombolysis Improves Outcome After Thrombotic Microembolism-Induced Acute Ischemic Stroke, *Stroke*, 2016, **47**(5), 1344–1353, DOI: 10.1161/STROKEAHA.115.012056.

25 Y. Birnbaum, Y. Luo, T. She Nagai, M. C. Fishbein, T. C. Peterson and S. Li, Noninvasive in vivo clot dissolution without a thrombolytic drug, *Circulation*, 1998, **97**(2), 130–134.

26 F. Xie, J. Slikkerveer, J. Lof, E. Unger, S. Radio, T. Mastunga and T. R. Porter, Coronary and microvascular thrombolysis with guided diagnostic ultrasound and microbubbles in acute ST segment elevation myocardial infarction, *J. Am. Soc. Echocardiogr.*, 2011, **24**(12), 1400–1408.

27 W. C. Culp, E. Erdem, P. K. Roberson and M. M. Husain, Microbubble potentiated ultrasound as a method of stroke therapy in a pig model: preliminary findings, *J. Vasc. Intervent. Radiol.*, 2003, **14**(11), 1433–1436.

28 A. Prabhakar and R. Banerjee, Nanobubble Liposome Complexes for Diagnostic Imaging and Ultrasound-Triggered Drug Delivery in Cancers: A Theranostic Approach, *ACS Omega*, 2019, **4**(13), 15567–15580.

29 L. Goel and X. Jiang, Advances in sonothrombolysis techniques using piezoelectric transducers, *Sensors*, 2020, **20**(5), 1288.

30 L. Goel, H. Wu, B. Zhang, J. Kim, P. A. Dayton, Z. Xu and J. Xiaoning, Nanodroplet-mediated catheter-directed sonothrombolysis of retracted blood clots, *Microsyst. Nanoeng.*, 2021, **7**(1), 3.

31 Y. Zhou, Z. Wang, H. Shen, H. Ran, P. Li, W. SOng, Z. Yang and H. Chen, Microbubbles from gas-generating perfluorohexane nanoemulsions for targeted temperature-sensitive ultrasonography and synergistic HIFU ablation of tumors, *Adv. Mater.*, 2013, **25**(30), 4123–4130.

32 P. Panwar, B. Pandey, P. C. Lakhera and K. C. Singh, Preparation, characterization, and in vitro release study of albendazole-encapsulated nanosize liposomes, *Int. J. Nanomed.*, 2010, **5**(1), 101–108.

33 B. Petit, E. Gaud, D. Colevret, M. Arditi, F. Yan, F. Tranquart and E. Alleman, *In vitro* sonothrombolysis of human blood clots with BR38 microbubbles, *Ultrasound Med. Biol.*, 2012, **38**(7), 1222–1233.

34 A. Prabhakar and R. Banarjee, Nanobubble liposome complexes for diagnostic imaging and ultrasound-triggered drug delivery in cancers: a theranostic approach, *ACS Omega*, 2019, **4**(14), 15567–15580.

35 L. Saba, S. S. Sanagala, S. K. Gupta, V. K. Koppula, M. Amer, M. Johri, *et al.* Ultrasound-based internal carotid artery plaque characterization using deep learning paradigm on a supercomputer: a cardiovascular disease/stroke risk assessment system, *Int. J. Card. Imaging*, 2021, **37**(5), 1511–1528.

36 S. Latha, D. Samiappan and R. Kumar, Carotid artery ultrasound image analysis: a review of the literature, *Proc. Inst. Mech. Eng., Part H*, 2020, **234**(5), 417–443.

37 Y. Zhu, L. Guan and Y. Mu, Combined low-frequency ultrasound and urokinase-containing microbubbles in treatment of femoral artery thrombosis in a rabbit model, *PLoS One*, 2016, **11**(12), e0168909.

38 J. Kim, R. M. DeRuiter, L. Goel, Z. Xu and P. A. Dayton, A comparison of sonothrombolysis in aged clots between low-boiling-point phase-change nanodroplets and microbubbles of the same composition, *Ultrasound Med. Biol.*, 2020, **46**(11), 3059–3068.

39 A. T. Brown, R. Flores, E. Hamilton, P. K. Roberson, M. J. Borelli and W. C. Pulp, Microbubbles improve sonothrombolysis in vitro and decrease hemorrhage *in vivo* in a rabbit stroke model, *Invest. Radiol.*, 2011, **46**(3), 202–207.

40 M. J. Borelli, W. Brien, E. Hamilton, M. L. Oelze, J. Wu, L. J. Bernock, S. Tung, H. Rokadia and W. C. Pulp, Influences of microbubble diameter and ultrasonic parameters on in vitro sonothrombolysis efficacy, *J. Vasc. Intervent. Radiol.*, 2012, **23**(12), 1677–1684.

41 X. Wang, H. Chen, Y. Chen, M. Ma, K. Zhang, F. Li, Y. Zheng, D. Zheng, Q. Wang and J. SHi, Perfluorohexane-encapsulated mesoporous silica nanocapsules as enhancement agents for highly efficient high intensity focused ultrasound (HIFU), *Adv. Mater.*, 2012, **24**(6), 785–791.